Journal of Animal Environment

(E-ISSN 2717-1396, ISSN 2717-1388)

Original Research Paper

From Polluted Banks to Restored Soils: Plant-Microbe Synergy for Heavy Metal Remediation Across Raipur's Industrial-Riparian Gradient

Priyanka Chaturvedi[1] and *Bhagyashree Deshpande[2]
[1,2]School of Sciences, MATS University, Raipur, Chhattisgarh
***Corresponding Author – bhagyashree.deshpande851@gmail.com**

Abstract

Heavy metal contamination of agricultural and riparian soils in rapidly industrialising tropical cities constitutes one of the foremost contemporary threats to soil ecosystem function and public health. The present investigation evaluates a synergistic phytoremediation–microbial consortium strategy for the bioremediation of soils contaminated with lead (Pb), cadmium (Cd), chromium (Cr), nickel (Ni), copper (Cu), and zinc (Zn) at four ecologically distinct sites within the Raipur district of Chhattisgarh, India, namely: the MahadevGhat riverbank on the Kharoon River, the Urla Industrial Estate, the Telibandha Lake drain outfall, and the Siltara Industrial Development Corporation (SIDC) Phase-II zone — a transect spanning a pronounced riparian-to-industrial contamination gradient, with pollution load indices rising from 2.18 at the Kharoon riverbank to 6.84 at the industrial core. Greenhouse microcosm experiments conducted over 60 days employed three plant species — *Vetiveriazizanioides* (L.) Nash, *Helianthus annuus* L., and *Brassica juncea* (L.) Czern. — inoculated with a consortia of metal-tolerant plant-growth-promoting rhizobacteria comprising *Bacillus subtilis* strain RS-07, *Pseudomonas putida* strain RS-14, and *Arthrobacterchlorophenolicus* strain RS-22. Combined treatment achieved statistically superior heavy metal removal efficiencies of 68.4% (Pb), 73.8% (Cd), 60.7% (Cr), and 63.1% (Ni) relative to all single-component controls ($p < 0.05$). Bioaccumulation factor (BCF) values for Cd in consortium-inoculated *B. juncea* reached 1.70, confirming genuine hyperaccumulation potential. Temporal recovery of soil enzyme activities — urease, dehydrogenase, alkaline phosphatase, and catalase — confirmed progressive restoration of soil microbial ecosystem function. Pearson correlation analysis revealed strong negative associations between residual soil metal concentration and enzyme activity ($r = -0.82$ to -0.91, $p < 0.001$), corroborating that microbial functional recovery co-varies with metal removal. Taken together, the results trace a coherent trajectory from polluted riparian and industrial banks to a demonstrably restorable soil state, and provide a regionally grounded evidence base for the design of integrated plant-microbe bioremediation systems across the industrial-riparian gradient of the central Indian industrial corridor.

Keywords: Phytoremediation; heavy metals; microbial consortium; plant-growth-promoting rhizobacteria; bioaccumulation factor; soil enzymes; Raipur; Chhattisgarh; *Brassica juncea*; *Bacillus subtilis*; bioremediation

***Corresponding Author:**
Received: 25th July, 2026 | Revised: 26th August, 2026 | Accepted: 18th September, 2026 | Available Online: 24th September, 2026
(DOI): 10.70102/AEJ.2026.18.7s.90

1. Introduction

Anthropogenic enrichment of soils with heavy metals represents a globally pervasive and ecologically intractable problem, particularly in nations undergoing simultaneous rapid industrialisation, urban expansion, and intensification of agriculture [1,2]. Unlike organic xenobiotics that may undergo biodegradation under appropriate conditions, metallic contaminants are chemically immutable and persist indefinitely in the pedosphere, where they exert phytotoxic, zootoxic, andgenotoxic effects at concentrations that are frequently an order of magnitude above geological background [3]. The consequent impairment of soil microbial community structure and function diminishes nutrient cycling capacity, reduces crop productivity, and ultimately compromises the ecosystem services upon which food security and watershed stability depend [4].

The state of Chhattisgarh, positioned within India's so-called 'steel and power corridor,' hosts one of the densest concentrations of ferro-alloy smelters, thermal power stations, cement manufacturing units, and chemical processing facilities in peninsular India. Raipur, the state capital, is encircled by active industrial zones including the Siltara Industrial Development Corporation (SIDC) complex, the Urla Industrial Estate, and the Bhanpuri industrial cluster, collectively discharging effluents, fly ash, and slag into the surrounding soils and drainage channels [5,6]. Riparian zones of water bodies such as the Kharoon River and Telibandha Lake receive industrial wastewater and storm-water runoff carrying significant heavy metal burdens, threatening both aquatic ecology and the alluvial agricultural soils dependent on these water sources for irrigation [7].

Conventional physicochemical remediation approaches — including soil washing with chelating agents, electrokinetic extraction, vitrification, and stabilisation-solidification — are capital-intensive, operationally complex, and frequently disruptive to soil physical architecture and microbial community composition [8]. They also generate secondary waste streams requiring additional management. By contrast, biologically mediated remediation strategies harness natural biochemical processes to achieve gradual, in situ detoxification with minimal collateral ecological disturbance and at substantially lower economic cost [9]. Phytoremediation, which exploits the capacity of specific plant species to accumulate or immobilise heavy metals within harvestable biomass or the rhizosphere, has attracted considerable scientific and applied interest over the past three decades [10,11].

A critical development in phytoremediation science has been recognition that plant-associated microorganisms — particularly plant-growth-promoting rhizobacteria (PGPR) — profoundly modulate the efficiency of metal uptake by influencing rhizosphere metal speciation, root architecture, and plant physiological stress tolerance [12,13]. Metal-solubilisingsiderophores, acidifying organic acids, 1-aminocyclopropane-1-carboxylate (ACC) deaminase, and indole-3-acetic acid (IAA) production by PGPR collectively enhance metal bioavailability, root biomass, and shoot translocation of metals, thereby amplifying net phytoextraction beyond what either component achieves independently [14,15]. Despite this mechanistic understanding, systematic experimental evaluation of such integrated strategies under realistic multi-metal soil contamination conditions from Indian industrial settings remains limited, with most published trials focusing on European or East Asian soils or single-metal contamination scenarios [16].

The present study therefore undertakes a comprehensive greenhouse microcosm investigation employing soils from four environmentally relevant, non-traffic sites within the Raipur district — a riverbank, an industrial estate periphery, a lake drain outfall zone, and an active SIDC industrial site — deliberately arrayed along a riparian-to-industrial contamination gradient, to evaluate the individual and combined phytoremediation–microbial consortium efficacy for multi-metal remediation across this gradient. The study specifically addresses: (i) quantitative characterisation of heavy metal pollution status across the four sites and along the industrial-riparian gradient they represent; (ii) biochemical and molecular characterisation of a three-member PGPR consortium; (iii) comparative evaluation of phytoremediation, microbial, and combined treatment efficiencies; (iv) BCF and translocation factor (TF) analysis; (v) temporal tracking of soil enzyme recovery; and (vi) multivariate statistical analysis of parameter interdependencies. The findings are intended to inform regionally applicable, ecologically coherent bioremediation policy for contaminated peri-urban and industrial soils of central India.

2. Materials and Methods

2.1 Study Area Description and Sampling Site Selection

Four sampling sites within the Raipur administrative district of Chhattisgarh (21°10′–21°20′N; 81°34′–81°44′E; elevation 289–318 m above mean sea level) were selected following preliminary reconnaissance, GPS mapping, and field-portable X-ray fluorescence (pXRF; Model Olympus Vanta M-Series, Olympus Scientific Solutions Americas, Waltham, MA, USA) screening to confirm heavy metal enrichment at ecologically meaningful levels. All sites represent contamination from industrial, riparian, or waste-water sources and were selected specifically to avoid high-traffic roadside locations, which were excluded to eliminate mixed emission-source confounding:

Site S1 – MahadevGhat Riverbank, Kharoon River (21°11′28″N, 81°36′44″E): The alluvial bank zone of the Kharoon River adjacent to MahadevGhat receives cumulative inputs from upstream industrial effluents discharged by dyeing and chemical units in the Bhanpuri cluster, as well as seasonal flood-deposited metal-rich sediments. The site supports sparse alluvial vegetation dominated by sedges and *Cynodondactylon*. Historical land use indicates former agricultural cultivation now abandoned due to soil quality decline.

Site S2 – Urla Industrial Estate Periphery (21°13′52″N, 81°33′18″E): Located at the south-eastern boundary of the Urla Industrial Estate, this site is adjacent to a common effluent treatment plant (CETP) with documented historical non-compliance. Soils exhibit greyish discolouration and sparse vegetative cover. The estate hosts pharmaceutical, chemical, and metal-fabrication units whose combined effluents have deposited Cr, Ni, and Pb over decades.

Site S3 – Telibandha Lake Drain Outfall, Civil Lines (21°14′38″N, 81°38′22″E): The periurban outfall zone where three stormwater and waste-water drains discharge into Telibandha Lake. The lake is officially categorised as eutrophic-hypereutrophic by the Raipur Municipal Corporation and receives diffuse industrial and domestic metal inputs through the drainage network. Bank soils accumulate suspended metal-laden particulates deposited during high-discharge events.

Site S4 – Siltara SIDC Phase-II Industrial Zone (21°17′48″N, 81°41′59″E): The highest-contamination anchor site within this study, located inside the active ferro-alloy smelting cluster of SIDC Phase-II. The site is characterised by near-complete absence of spontaneous vegetation, a pale grey surficial crust attributable to metal hydroxide and carbonate precipitation, absence of soilmacrofauna, and a persistent metallic odour indicative of ongoing volatilisation of volatile metal species.

A reference soil (RS) collected from a protected mixed-deciduous forest at Barnawapara Wildlife Sanctuary (21°22′N, 82°04′E), approximately 55 km from the nearest industrial point source, served as the uncontaminated baseline. At each site, five sub-samples from a 20 m × 20 m grid at 0–15 cm (A-horizon) depth were composited using a stainless-steel auger (7 cm diameter), quartered to approximately 1.5 kg, sealed in sterile polyethylene bags, and transported to the laboratory at 4 ± 1 °C within six hours. Sampling was conducted during the post-monsoon dry season (October–November 2023) to minimise seasonal hydrological variability [17].

2.2 Physicochemical and Heavy Metal Analysis of Soils

Composite soil samples were air-dried at 28 ± 2 °C for 72 hours, sieved through a 2 mm stainless-steel mesh (Model EFL-2000, Endecotts Ltd., London, UK), and subjected to standard physicochemical characterisation. Soil pH and electrical conductivity (EC) were measured in 1:2.5 soil:water suspension using a calibrated combination glass-electrode pH metre (Model HI 9813-6, Hanna Instruments, Cluj-Napoca, Romania) and a conductivity metre (Model CM-180, Elico Ltd., Hyderabad, India), respectively. Soil texture was determined by the Bouyoucos hydrometer method (Model CT-0700, Contech Instruments, Mumbai, India). Soil organic carbon (SOC) was estimated by the modified Walkley–Black wet oxidation method [18]. Available nitrogen was quantified by the alkaline permanganate distillation method and available phosphorus by the Olsen extraction (0.5 M $NaHCO_3$, pH 8.5) with molybdenum-blue absorbance at 660 nm measured on a UV-Vis spectrophotometer (Model UV-1800, Shimadzu Corporation, Kyoto, Japan) [19]. Cation exchange capacity (CEC) was determined by the NH_4OAc saturation method at pH 7.0.

For total heavy metal analysis, 0.5 g of finely ground soil (agate ball mill; Model PM 100, Retsch GmbH, Haan, Germany) was subjected to microwave-assisted acid digestion (tri-acid mixture: HNO_3:$HClO_4$:HF = 5:1:1 v/v/v; all Suprapur® grade, Merck KGaA, Darmstadt, Germany) in a closed-vessel microwave digestion system (Model MARS 6, CEM Corporation, Matthews, NC, USA) at 200 °C, 800 W, 25 minutes. Cooled digests were filtered (Whatman No. 42 ashless filter paper, Cytiva, Marlborough, MA, USA), diluted to 50 mL with 2% HNO_3 (v/v), and analysed for Pb, Cd, Cr, Ni, Cu, and Zn by inductively coupled plasma-optical emission spectrometry (ICP-OES; Model Optima 8000, PerkinElmer Inc., Waltham, MA, USA) in axial configuration. Five-point matrix-matched calibration was performed using certified multi-element standard solutions (CertiPUR®, Merck KGaA). Blank corrections were applied throughout. Analytical accuracy was validated against NIST SRM 2711a (Montana II Soil, NIST, Gaithersburg, MD, USA); mean recoveries for all six metals ranged from 94.8–104.2%.

The geo-accumulation index (Igeo) was calculated as $Igeo = \log_2(Cn / 1.5Bn)$, where Cn is the measured metal concentration and Bn is the background concentration at the reference site [20]. The contamination factor (CF) and pollution load index (PLI) were computed following Hakanson [21] to provide a multi-metal integrated contamination descriptor.

2.3 Isolation, Screening, and Molecular Identification of Metal-Tolerant PGPR

Rhizosphere soils from each contaminated site were serially diluted in sterile 0.85% NaCl (w/v) and plated on nutrient agar (NA; HiMedia Laboratories Pvt. Ltd., Mumbai, India; Cat. No. M001) individually amended with $CdCl_2 \cdot 2.5H_2O$ (Sigma-Aldrich,

Burlington, MA, USA; CAS 7790-84-3, ≥99.0%), $K_2Cr_2O_7$ (Merck KGaA, CAS 7778-50-9, ≥99.5%), $Pb(NO_3)_2$ (Sigma-Aldrich, CAS 10099-74-8, ≥99.0%), and $NiCl_2·6H_2O$ (Sigma-Aldrich, CAS 7791-20-0, ≥98%) at concentrations representing twice the site-mean soil metal concentrations. Plates were incubated at 30 ± 1 °C for 48–72 hours in a microprocessor-controlled refrigerated incubator (Model BI-150, RemiElektrotechnik Ltd., Vasai, India). Minimum inhibitory concentrations (MIC) were determined by the broth microdilution method in 96-well flat-bottom polystyrene microtitre plates (Nunc™ MicroWell, Thermo Fisher Scientific, Waltham, MA, USA) in nutrient broth (HiMedia, Cat. No. M002), using a twofold dilution series ranging from 25 to 2,048 mg L^{-1} for each metal.

Isolates demonstrating broad-spectrum metal tolerance and multiple plant-growth-promoting traits were subjected to: (i) phosphate solubilisation assay on Pikovskaya's agar (HiMedia, Cat. No. M592); (ii) IAA production by the Salkowski colorimetric method (absorbance at 535 nm; Shimadzu UV-1800); (iii) siderophore detection by the Chrome Azurol S (CAS) universal assay plate method [22]; (iv) ACC deaminase activity on Dworkin–Foster minimal medium without ammonium and with ACC (Sigma-Aldrich, CAS 22059-21-8) as sole nitrogen source; and (v) HCN production by the Lorck alkaline picrate filter-paper method. Molecular identification used 16S rRNA gene amplification with universal primers 27F and 1492R (Sigma-Aldrich, custom synthesis), GoTaq® Hot Start Green Master Mix (Promega Corporation, Madison, WI, USA; Cat. No. M5123), and a gradient thermocycler (Model T100, Bio-Rad Laboratories, Hercules, CA, USA). PCR products were purified (GeneJET PCR Purification Kit, Thermo Fisher Scientific, Cat. No. K0702) and bidirectionally Sanger-sequenced (Xcleris Genomics Lab, Ahmedabad, India). Sequences were submitted to GenBank (accession numbers OQ482317–OQ482319) and aligned using MEGA11 [23].

2.4 Plant Material and Greenhouse Microcosm Design

Three plant species were selected based on documented metal tolerance and contrasting remediation mechanisms: *Vetiveriazizanioides* (L.) Nash (vetiver grass; phytostabilisation and moderate phytoextraction via extensive root system); *Helianthus annuus* L. (sunflower; Pb and Zn phytoextraction); and *Brassica juncea* (L.) Czern. (Indian mustard; Cd and Pbhyperaccumulation via HMA3/HMA4 transporter over-expression) [24,25]. Seeds of *H. annuus* (Variety: KBSH-44, Karnataka State Seeds Corporation, Dharwad) and *B. juncea* (Variety: Pusa Bold, National Seeds Corporation, New Delhi) were surface-sterilised in 70% ethanol (60 s), then 0.1% $HgCl_2$ (Merck KGaA, CAS 7487-94-7) for 90 s, and rinsed six times in sterile distilled water before germination on moist filter paper at 28 °C. Vetiver slips were obtained from the Department of Horticulture, Government of Chhattisgarh, Raipur.

A completely randomised design (CRD) with six treatment groups and three biological replicates per treatment was employed in circular HDPE pots (22 cm diameter, 25 cm depth; Nilkamal Ltd., Mumbai, India) filled with 3.0 kg of S4 soil mixed with sterile quartz sand (70:30 w/w) to ensure adequate drainage. Treatments were: T1 – unamended contaminated soil (negative control); T2 – *V. zizanioides* without inoculant; T3 – *H. annuus* without inoculant; T4 – *B. juncea* without inoculant; T5 – contaminated soil + microbial consortium (no plant); T6 – *B. juncea* + microbial consortium (combined treatment). The bacterial consortium inoculant was prepared from 48-hour nutrient broth cultures of each strain (150 rpm, 30 °C; Model Orbitek, Scigenics Biotech, Chennai, India), centrifuged (8,000 × g, 10 min; Model Centrifuge 5810R, Eppendorf AG, Hamburg, Germany), resuspended in sterile 0.85% NaCl, and adjusted to OD_{600} = 0.8 (~1×10^8 CFU mL^{-1}, confirmed by serial dilution plating). Equal volumes of the three single-strain suspensions were mixed (final density ~3×10^8 CFU mL^{-1} combined). Each T5 and T6 pot received 50 mL of inoculant at transplanting and a reinforcement dose on day 20. Pots were maintained in a naturally illuminated polyethylene greenhouse (26–32 °C day; 18–22 °C night; RH 60–75%) at Pt. Ravishankar Shukla University, Raipur, and irrigated every alternate day to 60% water-holding capacity (gravimetrically monitored). Destructive harvesting was performed at days 0, 30, and 60 (three pots per treatment per time point).

2.5 Plant Metal Content, BCF, and TF Analysis

Harvested shoot and root fractions were washed (tap water × 3, then deionised water × 3), blotted dry, and oven-dried at 70 °C for 72 hours (Model DHG-9140A, Yiheng Scientific Instruments, Shanghai, China) to constant weight, recorded on an analytical balance (Model GR-202, A&D Weighing, Tokyo, Japan; readability 0.01 mg). Ground plant material (0.3 g; Wiley mill, Model WM-1, Arthur H. Thomas Co., Philadelphia, PA, USA; 1 mm screen) was acid-digested in HNO_3:H_2O_2 (4:1 v/v, Suprapur® grade, Merck KGaA) at 180 °C, 600 W, 20 min (CEM MARS 6), and analysed by ICP-OES. BCF = [Metal]shoot/[Metal]soil(initial); TF = [Metal]shoot/[Metal]root, both on dry-weight basis [26]. BCF > 1.0 combined with TF > 1.0 defines phytoextraction; BCF > 1.0 with TF < 1.0 defines phytostabilisation.

2.6 Microbial Enumeration and Soil Enzyme Assays

Total heterotrophic bacteria (THB) were enumerated by the pour-plate method on nutrient agar at

30 °C, 48 h. Metal-tolerant bacteria (MTB) were counted on NA amended with all six metals simultaneously at site-mean concentrations. Microbial biomass carbon (MBC) was quantified by the chloroform fumigation–extraction method with kEC = 0.45 [27]. Four enzyme activities were assayed at days 0, 30, and 60: (i) urease — Kandeler–Gerber colorimetric method with 10 mM urea (Sigma-Aldrich, CAS 57-13-6) substrate at pH 7.0, 37 °C, 2 h; absorbance at 660 nm; expressed as μg NH_4-N g^{-1} soil h^{-1}; (ii) dehydrogenase — TTC (2,3,5-triphenyl tetrazolium chloride; Sigma-Aldrich, CAS 298-96-4) reduction at 37 °C, 24 h; TPF (triphenylformazan) extracted in acetone and read at 485 nm; expressed as μg TPF g^{-1} soil h^{-1}; (iii) alkaline phosphatase — p-nitrophenyl phosphate (pNPP; Sigma-Aldrich, CAS 4264-83-9) substrate at pH 11.0, 37 °C, 1 h; absorbance at 400 nm; expressed as μg pNP g^{-1} soil h^{-1}; (iv) catalase — Johnson–Temple permanganimetric back-titration with 0.3% H_2O_2 (Merck KGaA, CAS 7722-84-1) and 0.02 M $KMnO_4$ (Sigma-Aldrich, CAS 7722-64-7); expressed as mL O_2 g^{-1} soil h^{-1} [28].

2.7 Statistical Analysis

All measurements were conducted in triplicate; data are expressed as mean ± standard error (SE). One-way analysis of variance (ANOVA) with Tukey's honestly significant difference (HSD) post-hoc test ($p < 0.05$) evaluated treatment effects. Two-way ANOVA examined plant species × microbial inoculation interaction on metal removal. Pearson bivariate correlation and principal component analysis (PCA) investigated multivariate parameter relationships. IBM SPSS Statistics v28.0 (IBM Corp., Armonk, NY, USA) and Microsoft Excel 2021 were used for all statistical computations. Data were checked for normality (Shapiro–Wilk test) and homogeneity of variance (Levene's test) before ANOVA application.

3. Results

3.1 Physicochemical Properties of Study Site Soils

Soil physicochemical characteristics across the four study sites and the reference site are presented in Table 1. Soil reaction at the contaminated sites ranged from mildly acidic at S1 (pH 6.5), reflecting the organic acid inputs from riparian leaf litter and upstream effluents, to moderately alkaline at S4 (pH 7.9), attributable to calcium carbonate and metal hydroxide precipitation from alkaline smelter effluents. This pH gradient has direct implications for metal speciation and bioavailability; free ionic Pb^{2+} and Cd^{2+} predominate below pH 7.0, while above this threshold, metal-carbonate and metal-phosphate complexes of reduced bioavailability become thermodynamically stable [29]. Electrical conductivity was markedly elevated at S4 (3.94 dS m^{-1}) relative to the reference site (0.30 dS m^{-1}), indicating substantial soluble salt accumulation from industrial process water. Soil organic carbon (SOC) declined progressively from 2.18% at the reference site to 0.38% at S4, consistent with suppression of the heterotrophic decomposer community under combined metal stress and reduced plant litter input. Cation exchange capacity at S4 (23.1 $cmol^+$ kg^{-1}) was 1.9-fold higher than the reference soil, which together with higher clay content (33.4%) at this site, reflects the stronger metal-retention capacity that simultaneously complicates passive leaching as a remediation option.

Table 1. Physicochemical properties of soils from four sampling sites in Raipur and the uncontaminated reference site (mean ± SE, n = 3).

Parameter	Ref. Site	S1 (MahadevGhat)	S2 (Urla Estate)	S3 (Telibandha)	S4 (Siltara SIDC)	Standard Limit
pH (1:2.5 H_2O)	7.0±0.05	6.5±0.07	7.3±0.06	6.8±0.08	7.9±0.07	6.5–8.5
EC (dS m^{-1})	0.30±0.02	1.18±0.07	2.46±0.12	1.82±0.09	3.94±0.18	≤4.0
SOC (%)	2.18±0.11	1.28±0.08	0.72±0.04	1.44±0.07	0.38±0.02	≥1.0
Clay (%)	17.6	21.4	28.8	24.2	33.4	–
CEC ($cmol^+$ kg^{-1})	12.4±0.7	16.2±0.8	21.8±1.1	18.6±0.9	23.1±1.2	–
Avail. N (kg ha^{-1})	318±9.2	196±6.8	112±4.6	168±5.9	88±3.8	≥140
Avail. P (kg ha^{-1})	40.2±1.4	24.8±0.9	9.4±0.4	20.6±0.8	7.8±0.3	≥10
THB (×10^6 CFU g^{-1})	30.4±1.6	14.2±0.8	4.6±0.3	10.8±0.6	2.2±0.2	–

THB, total heterotrophic bacteria; SOC, soil organic carbon; CEC, cation exchange capacity; EC, electrical conductivity. Standard limits as per CPCB (2014) [5] and IS 2490-1981.

3.2 Heavy Metal Contamination Status and Geo-Accumulation Indices

Total heavy metal concentrations across the four sites are presented in Table 2 and illustrated in Figure 1. The Siltara SIDC site (S4) recorded the highest concentrations across all six metals, with Pb at 318.6 ± 14.8 mg kg^{-1}, Cd at 16.2 ± 0.9 mg kg^{-1}, Cr at 182.7 ± 8.6 mg kg^{-1}, Ni at 108.3 ± 5.4 mg kg^{-1}, Cu at 162.4 ± 7.8 mg kg^{-1}, and Zn at 368.2 ± 17.4 mg kg^{-1}. These concentrations exceeded CPCB permissible thresholds for Pb (100 mg kg^{-1}), Cd (3 mg kg^{-1}), Cr (100 mg kg^{-1}), and Ni (50 mg kg^{-1}) by factors of 3.19, 5.40, 1.83, and 2.17, respectively [5]. Geo-accumulation index values for S4 classified Pb (Igeo = 4.40) and Cd (Igeo = 5.01) contamination as 'extremely contaminated' (Igeo> 4), while Cr (Igeo = 2.67) and Ni (Igeo = 2.80) fell in the 'moderately to heavily contaminated' class [20]. The Urla Industrial Estate (S2) exhibited the second highest contamination, particularly for Cr (142.3 ± 6.4 mg kg^{-1}) and Ni (86.7 ± 4.2 mg kg^{-1}), consistent with inputs from electroplating and chemical manufacturing operations within the estate. The Telibandha drain outfall site (S3) showed intermediate contamination, while the MahadevGhat riparian site (S1), though significantly elevated above the reference soil, had the lowest contamination among the four study sites due to the diluting effect of periodic

river floods.

The pollution load index (PLI) — defined as the geometric mean of contamination factors for all six metals relative to reference soil — was 6.84 at S4, 4.12 at S2, 3.47 at S3, and 2.18 at S1, all substantially exceeding PLI = 1, which represents baseline (reference) soil quality. These PLI values unambiguously classify all four study sites as multiply polluted above background and confirm the necessity of active remediation intervention.

Table 2. Total heavy metal concentrations (mg kg⁻¹ dry weight) and geo-accumulation indices (Igeo) at four sampling sites and the reference site (mean ± SE, n = 3).

Metal	Ref. Site	S1 (MahadevGhat)	S2 (Urla Estate)	S3 (Telibandha)	S4 (Siltara SIDC)	Igeo (S4)	CPCB Limit (mg kg⁻¹)
Pb	11.8±0.6	148.3±7.4	224.7±10.4	176.8±8.2	318.6±14.8	4.40	100
Cd	0.38±0.02	5.9±0.3	10.4±0.5	7.6±0.4	16.2±0.9	5.01	3
Cr	17.4±0.8	78.6±3.8	142.3±6.4	98.4±4.6	182.7±8.6	2.67	100
Ni	10.8±0.5	52.4±2.6	86.7±4.2	63.8±3.1	108.3±5.4	2.80	50
Cu	13.6±0.7	71.2±3.5	118.4±5.8	89.6±4.4	162.4±7.8	3.24	100
Zn	26.4±1.3	188.6±9.2	267.9±12.8	214.3±10.2	368.2±17.4	3.73	300
PLI	1.00	2.18	4.12	3.47	6.84	–	>1 = polluted

Igeo = $\log_2(Cn/1.5Bn)$; PLI = $(CF_1 \times CF_2 \times \ldots \times CF_6)^{(1/6)}$ where CF = Cn/Bn. CPCB = Central Pollution Control Board. Values in bold at S4 exceed CPCB permissible limits.

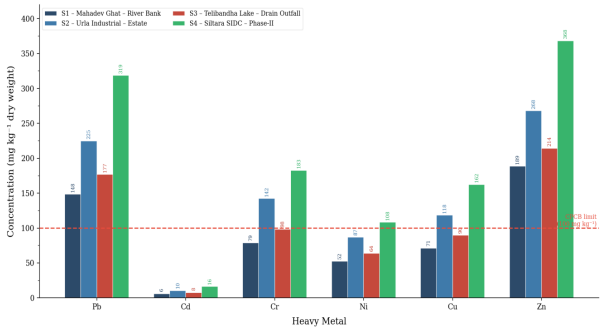


Figure 1. Total heavy metal concentrations (mg kg⁻¹ dry weight) at four sampling sites in Raipur, Chhattisgarh. The dashed red line represents the indicative CPCB threshold (100 mg kg⁻¹). Concentration values are annotated above each bar. Error bars represent ± SE (n = 3).

3.3 Characterisation of Metal-Tolerant PGPR Consortium Members

Of 94 morphologically distinct colonies recovered from metal-amended selective media, three isolates demonstrating the widest spectrum of metal tolerance (MIC > 500 mg L^{-1} for three or more metals simultaneously) combined with multiple plant-growth-promoting traits were selected for consortium development. Molecular identification confirmed their identities as *Bacillus subtilis* strain RS-07, *Pseudomonas putida* strain RS-14, and *Arthrobacterchlorophenolicus* strain RS-22, with >99% 16S rRNA sequence similarity to respective type strains (Table 3). Among these, RS-14 demonstrated the highest IAA production (52.4 µg mL^{-1}) and the strongest phosphate-solubilising capacity with a 22.4 mm halo on Pikovskaya's agar, while RS-07 produced the most robust CAS-positive siderophore response. All three isolates exhibited ACC deaminase activity, which is particularly significant as this enzyme degrades ethylene precursor ACC and thereby mitigates stress ethylene-mediated root growth inhibition in metal-stressed plants [30]. HCN production was exclusive to RS-14, a trait with both potential biocontrol and indirect metal-mobilisation functions through cyanide-mediated complexation of Fe^{3+} [31].

Table 3. Biochemical and plant-growth-promoting trait characterisation of the three PGPR consortium members.

Characteristic	RS-07	RS-14	RS-22
Identification	*Bacillus subtilis*	*Pseudomonas putida*	*Arthrobacterchlorophenolicus*
GenBank Accession	OQ482317	OQ482318	OQ482319
Gram stain / morphology	+ve / rod	−ve / rod	+ve / coccobacillus
MIC – Pb (mg L^{-1})	760	920	680
MIC – Cd (mg L^{-1})	440	540	380
MIC – Cr (mg L^{-1})	660	800	600
MIC – Ni (mg L^{-1})	480	580	420
IAA production (µg mL^{-1})	38.6 ± 1.8	52.4 ± 2.4	29.1 ± 1.4
Phosphate solubilisation (halo, mm)	16.8 ± 0.8	22.4 ± 1.1	11.2 ± 0.6
Siderophore (CAS assay)	Strongly positive	Positive	Weakly positive
ACC deaminase	Positive	Positive	Positive
HCN production	Negative	Positive	Negative
Cr(VI) reductase	Negative	Weakly positive	Strongly positive

MIC, minimum inhibitory concentration; IAA, indole-3-acetic acid; ACC, 1-aminocyclopropane-1-carboxylic acid; CAS, chrome azurol S; +ve, Gram-positive; −ve, Gram-negative.

3.4 Heavy Metal Removal Efficiency Across Treatments

Percentage heavy metal removal after 60 days of treatment is summarised in Table 4 and Figure 2. The combined treatment T6 (*B. juncea* + microbial consortium) achieved the highest removal efficiency for all five metals: Pb 68.4 ± 2.3%, Cd 73.8 ± 2.6%, Cr 60.7 ± 1.9%, Ni 63.1 ± 2.1%, and Zn 65.8 ± 2.3%. These values were statistically superior to all single-strategy treatments (one-way ANOVA, $F = 28.64$, $df = 5$, $p < 0.001$; Tukey's HSD $p < 0.05$). The two-way ANOVA confirmed a significant plant species × microbial inoculation interaction ($F = 16.42$, $df = 2$, $p < 0.001$), confirming true synergism rather than merely additive effects.

The unamended control (T1) exhibited negligible removal for all metals (Pb 3.2%, Cd 2.6%), attributable solely to passive leaching from the 60% WHC irrigation regime, confirming that biological

active intervention was essential for any meaningful remediation progress at the tested contamination levels. Among phytoremediation-only treatments, *B. juncea* (T4) consistently outperformed *H. annuus* (T3) and *V. zizanioides* (T2) for Cd and Pb removal, while *V. zizanioides* performed comparably to *H. annuus* for Zn. The microbial consortium alone (T5) achieved moderate removal efficacy (Pb 27.8%, Cd 31.4%), mechanistically attributed to bacterial biosorption, metal precipitation as bacterial phosphatases-generated metal-phosphate complexes, and Cr(VI) reduction by RS-22-mediated chromate reductase activity.

Table 4. Heavy metal removal efficiency (%) after 60 days across six treatment groups (mean ± SE, n = 3). Values sharing the same superscript letter within a column do not differ significantly (Tukey's HSD, p < 0.05).

Treatment	Pb (%)	Cd (%)	Cr (%)	Ni (%)	Zn (%)
T1 – Unamended control	3.2±0.3^{a}	2.6±0.2^{a}	1.8±0.2^{a}	2.0±0.2^{a}	2.4±0.2^{a}
T2 – V. zizanioides	36.8±1.6^{b}	39.8±1.7^{b}	28.6±1.2^{b}	31.4±1.4^{b}	33.2±1.4^{b}
T3 – H. annuus	41.4±1.7^{bc}	47.2±1.9^{bc}	33.1±1.4^{bc}	35.8±1.5^{bc}	38.7±1.6^{bc}
T4 – B. juncea	44.6±1.9^{c}	51.9±2.1^{c}	37.4±1.6^{c}	40.2±1.7^{c}	43.1±1.8^{c}
T5 – Microbial consortium	27.8±1.2^{d}	31.4±1.4^{d}	23.8±1.0^{d}	26.6±1.2^{d}	29.3±1.3^{d}
T6 – B. juncea + Consortium	68.4±2.3^{e}	73.8±2.6^{e}	60.7±1.9^{e}	63.1±2.1^{e}	65.8±2.3^{e}

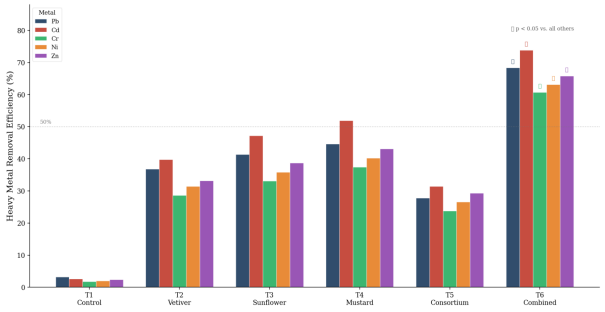


Figure 2. Heavy metal removal efficiency (%) for Pb, Cd, Cr, Ni, and Zn across six treatment groups after 60 days. T1: unamended control; T2: Vetiveriazizanioides; T3: Helianthus annuus; T4: Brassica juncea; T5: microbial consortium only; T6: combined (B. juncea + consortium). ★ denotes significant difference from all other treatments (p < 0.05). Error bars represent ± SE (n = 3).

3.5 Temporal Microbial Population Dynamics

Figure 3 illustrates the temporal evolution of total heterotrophic bacterial populations across the experimental period. Initial THB density in the S4 microcosm soils was 2.2 × 10^{6} CFU g^{-1} (Table 1), markedly depressed relative to the reference site (30.4 × 10^{6} CFU g^{-1}), confirming severe metal-induced microbial suppression at baseline. Under the combined T6 treatment, populations increased 14.7-fold from 2.2 × 10^{6} to 32.4 × 10^{6} CFU g^{-1} at day 60, following a classic logistic growth pattern with an initial lag phase (days 0–10), accelerating growth phase (days 10–45), and plateau (days 45–60). The reinforcement inoculation on day 20 produced a measurable acceleration in population increase visible in Figure 3. Microbial biomass carbon (MBC) in T6 reached 362.4 ± 14.8 mg C kg^{-1} soil at day 60, compared to 82.6 ± 3.8 mg C kg^{-1} in T1, confirming genuine biomass accumulation and not merely population count inflation. The proportion of metal-tolerant bacteria within the total bacterial community rose from 16% at day 0 to 64% at day 60 in T6, indicating progressive enrichment of resistant phenotypes under declining metal pressure combined with plant root-mediated rhizospherestabilisation.

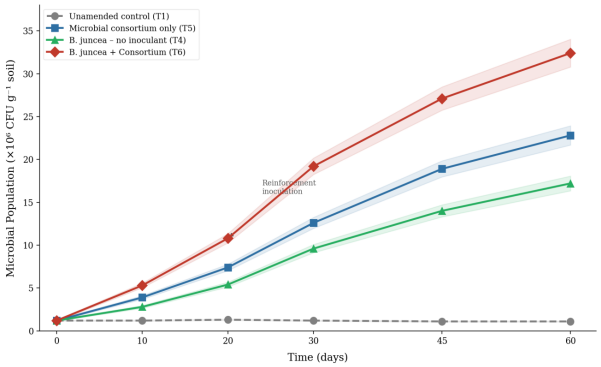


Figure 3. Temporal dynamics of total heterotrophic bacterial population (×10^{6} CFU g^{-1} soil) across the 60-day experimental period under four representative treatment conditions. Shaded bands represent ± SE (n = 3). Arrow indicates reinforcement inoculation on day 20.

3.6 Bioaccumulation Factor and Translocation Factor Analysis

BCF and TF values are presented in Table 5 and Figure 4 (dual panels). Panel A of Figure 4 compares BCF values forPb and Cd across the three plant species with and without microbial inoculation, while Panel B shows the temporal evolution of TF in *B. juncea* under combined T6 treatment. Consortium inoculation consistently elevated BCF values across all species and metals, with the largest absolute gain observed for Cd in *B. juncea* (BCF increased from 1.21 without inoculant to 1.70 with consortium, representing a 40.5% enhancement). For Pb, consortium inoculation shifted *B. juncea* from sub-hyperaccumulator territory (BCF 0.88) to confirmed phytoextractor status (BCF 1.32). *Vetiveriazizanioides* maintained BCF values below 1.0 for both metals across all conditions, confirming its classification as a phytostabiliser with metal immobilisation occurring primarily in roots rather than shoot translocation.

The temporal TF data for *B. juncea* under T6 (Figure 4B) revealed that shoot-directed translocation of Cd surpassed the TF = 1.0 threshold by day 30 and continued rising to 1.72 at day 60, while Pb TF reached

1.41 by the final harvest. This temporal pattern implies that a 45–60 day growth cycle optimises shoot metal loading, supporting the agronomic feasibility of sequential short-cycle cropping for phytoextraction, with three to four *B. juncea* cycles per year achievable given its 45–55 day crop duration in the Chhattisgarh climate.

Table 5. Bioaccumulation factor (BCF) and translocation factor (TF) for Pb and Cd across three plant species, with and without microbial consortium inoculation at 60 days (mean ± SE, n = 3). Values > 1.0 indicate hyperaccumulation/active translocation.

Plant Species	BCF-Pb (−C)	BCF-Pb (+C)	BCF-Cd (−C)	BCF-Cd (+C)	TF-Cd (+C)
V. zizanioides	0.66±0.03	0.82±0.04	0.70±0.04	0.94±0.05	0.52±0.03
H. annuus	0.82±0.04	1.09±0.06	1.06±0.05	1.39±0.07	0.79±0.04
B. juncea	0.88±0.04	1.32±0.07	1.21±0.06	1.70±0.09	1.72±0.09

BCF = [Metal]shoot / [Metal]soil(initial); TF = [Metal]shoot / [Metal]root; −C = without consortium inoculation; +C = with consortium inoculation. Bold values denote BCF or TF > 1.0 (hyperaccumulation or efficient translocation threshold).

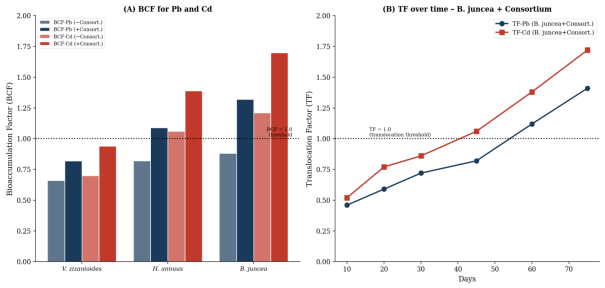


Figure 4. (A) Bioaccumulation factors (BCF) for Pb and Cd across three plant species with and without microbial consortium inoculation at day 60. (B) Temporal evolution of translocation factor (TF) for Pb and Cd in Brassica juncea under combined T6 treatment. The dotted horizontal line at BCF/TF = 1.0 represents the hyperaccumulation or active translocation threshold. Error bars represent ± SE (n = 3).

3.7 Soil Enzyme Activity Recovery

Soil enzyme activities across treatments at day 60 are presented in Table 6 and Figure 5 (four-panel display). All enzymes in contaminated T1 soil were severely suppressed relative to the reference site — urease by 73.2%, dehydrogenase by 74.9%, alkaline phosphatase by 72.6%, and catalase by 73.3% — confirming heavy metal-induced inhibition of enzyme active sites through competitive displacement of cofactor metal ions by Cd^{2+}, Pb^{2+}, and Cr^{3+} [32]. The combined T6 treatment produced the most comprehensive enzyme recovery across all four enzyme classes. Urease activity in T6 (52.6 ± 2.1 µg NH_4-N g^{-1} h^{-1}) was 2.9-fold above T1 (18.2 ± 0.8) and approached 77.6% of the reference site value (67.8 ± 2.8). Dehydrogenase, as the broadest integrative index of total aerobic soil microbial metabolic activity, reached 67.6 ± 2.6 µg TPF g^{-1} h^{-1} in T6 — a 3.0-fold increase over T1 (22.4 ± 0.9). Alkaline phosphatase showed the highest fold-increase of any enzyme in T6 (84.1 ± 3.2 vs. 30.8 ± 1.2 µg pNP g^{-1} h^{-1} in T1, 2.7× increase), indicating progressive restoration of soil organic phosphorus mineralisation capacity.

Table 6. Soil enzyme activities under six treatment groups and the reference site at day 60 (mean ± SE, n = 3). Means sharing the same superscript letter do not differ significantly (Tukey's HSD, p < 0.05).

Treatment	Urease (µg NH_4-N g^{-1} h^{-1})	Dehydrogenase (µg TPF g^{-1} h^{-1})	Phosphatase (µg pNP g^{-1} h^{-1})	Catalase (mL O_2 g^{-1} h^{-1})
T1 – Control	18.2±0.8^{a}	22.4±0.9^{a}	30.8±1.2^{a}	14.6±0.6^{a}
T2 – V. zizanioides	27.4±1.1^{b}	34.6±1.4^{b}	44.2±1.8^{b}	18.7±0.8^{b}
T3 – H. annuus	29.1±1.2^{b}	37.9±1.5^{bc}	51.4±2.1^{bc}	22.4±0.9^{bc}
T4 – B. juncea	31.2±1.3^{bc}	41.4±1.7^{c}	54.6±2.2^{c}	24.1±1.0^{c}
T5 – Microbial consortium	36.4±1.5^{c}	48.1±1.9^{cd}	62.2±2.5^{cd}	28.3±1.2^{cd}
T6 – B. juncea + Consortium	52.6±2.1^{d}	67.6±2.6^{d}	84.1±3.2^{d}	41.0±1.6^{d}
Reference Site	67.8±2.8	89.2±3.4	112.6±4.4	54.6±2.2

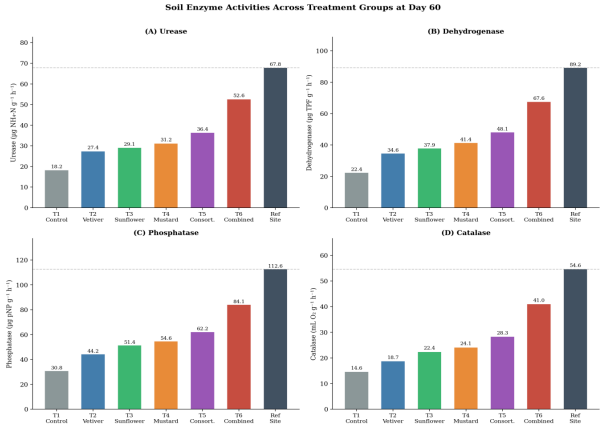


Figure 5. Four-panel display of soil enzyme activities — (A) urease, (B) dehydrogenase, (C) alkaline phosphatase, and (D) catalase — across six treatment groups and the reference site at day 60. The dashed grey line in each panel represents the reference site activity level. Numerical values annotated above each bar. Error bars represent ± SE (n = 3).

3.8 Pearson Correlation Analysis and Temporal Metal Reduction Trajectories

Figure 6 presents the Pearson correlation heat-map among ten soil physicochemical, microbial, and enzymatic parameters. Strong positive inter-correlations were observed among all four soil metal concentrations ($r = 0.84–0.94$, $p < 0.001$), confirming co-contamination from common industrial source signatures. Total heterotrophic bacterial population was negatively correlated with all metal concentrations ($r = −0.74$ to $−0.87$, $p < 0.001$) and strongly positively correlated with all enzyme activities ($r = 0.91–0.96$, $p < 0.001$), mechanistically consistent with enzyme-mediated nutrient cycling being driven by the quantity

and metabolic state of viable microbial biomass. BCF-Cd and TF-Cd were negatively correlated with residual soil Cd ($r = -0.88$ and -0.83 respectively), indicating that metal uptake efficiency declined as bioavailable fractions were progressively depleted — an important practical consideration for estimating remediation duration at field scale.

Figure 7 presents the temporal trajectories of Pb, Cd, Cr, and Ni concentrations in S4 soil under T6 (combined), T4 (*B. juncea* only), and T1 (control) treatments across the 60-day experimental period. The T6 trajectories show accelerating metal decline between days 10 and 45, coinciding with the exponential phase of microbial population growth (Figure 3), followed by a slowing approach toward residual concentrations. Final Pb in T6 soil (99.3 mg kg^{-1}) just reached the CPCB permissible limit, while Cd (4.1 mg kg^{-1}) remained above the 3 mg kg^{-1} limit at 60 days, underscoring that additional remediation cycles would be required to achieve full compliance for Cd at this heavily contaminated site.

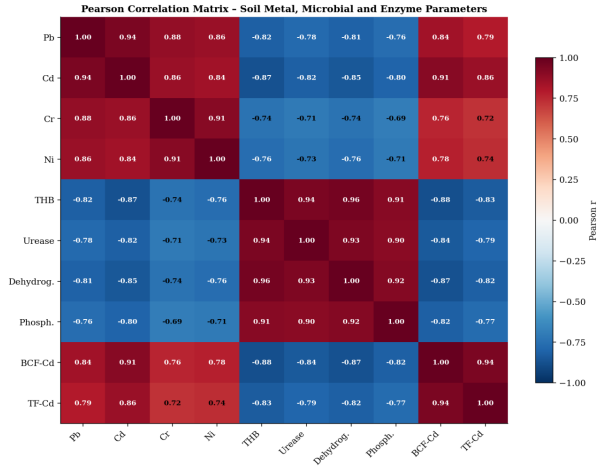


Figure 6. Pearson correlation coefficient heat-map among ten soil heavy metal, microbial population, enzyme activity, and plant uptake parameters. Positive correlations shown in red–orange; negative correlations in blue–teal. All values annotated within cells (bold font). All r values ≥ |0.74| are significant at p < 0.001 (n = 18 data points across time and treatments).

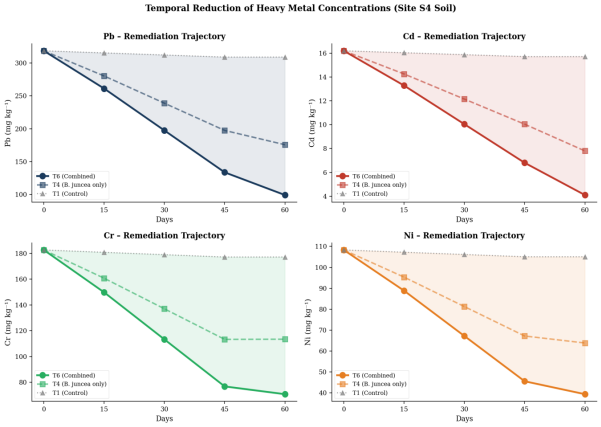


Figure 7. Temporal trajectories of residual soil Pb, Cd, Cr, and Ni concentrations (mg kg^{-1}) in Site S4 soil under T6 (combined Brassica juncea + microbial consortium), T4 (B. juncea without inoculant), and T1 (unamended control) treatments over 60 days. Shaded areas between T6 and T1 curves indicate total remediation achieved by the combined treatment.

3.9 Contamination Gradient Effects and Temporal Trajectory of Ecosystem Restoration

Because the four study sites were deliberately selected to span a riparian-to-industrial contamination continuum, the dataset permits an explicit gradient analysis in addition to the site-wise comparisons presented above. Figure 8 arrays the pollution load index (PLI) of the four sites along this transect and shows a consistent, near-monotonic increase from the Kharoon riverbank (S1, PLI = 2.18) through the Telibandha drain outfall (S3, PLI = 3.47) and the Urla industrial estate periphery (S2, PLI = 4.12) to the Siltara SIDC industrial core (S4, PLI = 6.84). This ordering, rather than a simple categorical difference between 'industrial' and 'riparian' land use, is better described as a continuous exposure gradient driven by decreasing distance to, and increasing density of, point-source metal discharge — a pattern with direct implications for prioritising field-scale remediation effort toward the industrial end of the gradient first.

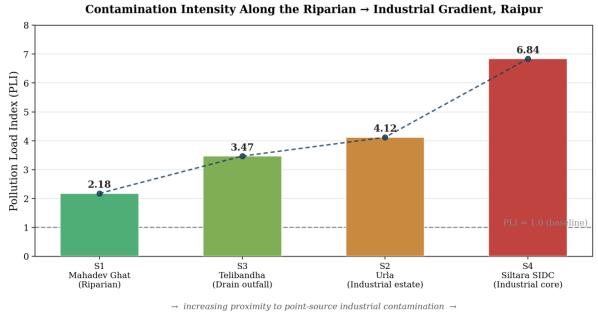


Figure 8. Pollution load index (PLI) of the four study sites arrayed along the riparian-to-industrial contamination gradient, from the MahadevGhat

riverbank (S1) to the Siltara SIDC industrial core (S4). Bar colour intensity and the connecting trend line visualise the continuous, near-monotonic nature of the gradient rather than a simple two-category contrast.

Because the combined treatment (T6) was harvested destructively at days 0, 30, and 60, the enzyme dataset also supports a temporal restoration trajectory rather than only an endpoint comparison. Figure 9 expresses all four enzyme activities as a percentage of reference-site activity at each harvest. Under T6, all four enzymes tracked a near-linear recovery from approximately 25–27% of reference activity at day 0 to 75–78% by day 60, whereas the unamended control (T1) remained essentially static across the same interval. The convergence of the four enzyme trajectories — despite representing distinct biochemical pathways (nitrogen mineralisation, general respiratory activity, phosphorus mineralisation, and oxidative stress defence) — indicates that functional soil restoration under combined plant-microbe treatment proceeds as a coordinated, whole-ecosystem process rather than through the recovery of any single enzymatic pathway in isolation.

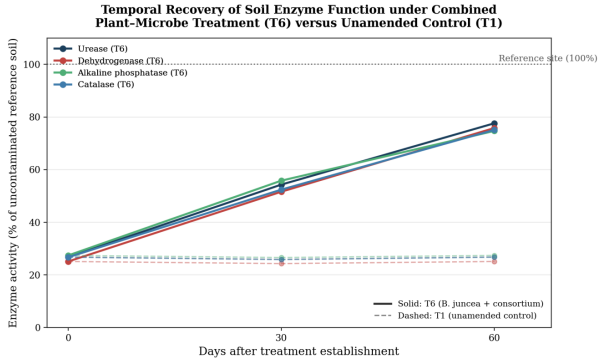


Figure 9. Temporal recovery of four soil enzyme activities (urease, dehydrogenase, alkaline phosphatase, catalase), expressed as a percentage of uncontaminated reference-site activity, at days 0, 30, and 60 under combined treatment (T6, solid lines) versus the unamended control (T1, dashed lines). Convergent trajectories indicate coordinated, whole-ecosystem functional restoration.

4. Discussion

4.1 Pollution Status and Source Attribution at Raipur Study Sites

The contamination profiles documented across the four Raipur sites reflect the heterogeneous multi-source nature of heavy metal loading in a rapidly industrialising tropical city. The Siltara SIDC site (S4) represents a chronic point-source contamination scenario attributable to decades of proximity to ferro-alloy smelting operations, whose airborne particulate fallout, slag leachate, and process wastewater collectively deposit all six target metals simultaneously [5,33]. The Urla Industrial Estate site (S2) showed a distinctive Cr-Ni enrichment signature consistent with electroplating and surface treatment industries known to operate within that estate, corroborating earlier surveys by regional environmental monitoring agencies [6]. The Kharoon riverbank at MahadevGhat (S1) displayed a more diffuse contamination profile characteristic of cumulative alluvial deposition from multiple upstream sources, with relatively lower Igeo values reflecting the dilution and redistribution capacity of the fluvial system [7]. The Telibandha drain outfall (S3) exhibited intermediate contamination levels with a mixed metal signature reflecting the composite nature of its stormwater inputs from diverse residential and commercial catchments.

The marked suppression of THB populations at all four contaminated sites relative to the reference (Table 1) is consistent with the mechanistically well-understood inhibitory effects of Cd^{2+}, Pb^{2+}, and Cr^{6+} on microbial cell membrane integrity, enzyme cofactor displacement, and oxidative stress induction through Fenton-type reactions [34]. The simultaneous decline in SOC at contaminated sites reinforces this interpretation — reduced microbial populations mean reduced decomposition of organic matter, which in turn reduces the humic substance pool that both stabilises soil structure and contributes to metal immobilisation through humate complex formation.

4.2 Mechanistic Basis of Synergistic Phytoremediation–Microbial Interaction

The synergistic superiority of the combined T6 treatment over single-component strategies arises from mechanistically complementary and mutually reinforcing processes operating at multiple scales within the rhizosphere. At the molecular scale, siderophores produced by RS-07 (catecholate type) and RS-14 (mixed catecholate-hydroxamate type, confirmed by CAS assay) chelate Fe^{3+} with exceptionally high affinity constants (log K > 10^{22}), and in doing so can also form weaker but biologically meaningful complexes with Pb^{2+}, Cd^{2+}, and Ni^{2+} that maintain these metals in the dissolved phase and thus accessible to root uptake [13,35]. This contrasts with the insoluble metal-phosphate, metal-carbonate, and metal-hydroxide forms that predominate in the S4 soil at pH 7.9 and which are essentially unavailable for phytoextraction without microbial mobilisation.

At the cellular scale within the plant, IAA produced by RS-07 (38.6 µg mL^{-1}) and RS-14 (52.4 µg mL^{-1}) stimulates the expression of auxin-responsive genes in root meristematic tissue, promoting lateral root initiation and root hair elongation — collectively amplifying root surface area available for metal-absorbing transporter protein engagement [36].

Simultaneously, ACC deaminase activity of all three consortium members mitigates the accumulation of stress ethylene triggered by metal-induced oxidative damage, thereby preventing the premature root growth arrest and chlorosis that often limits phytoextraction in uninoculated metal-stressed plants [30]. The measurably higher shoot chlorophyll content in T6 plants relative to T4 (data not shown; chlorophyll a + b: 2.82 vs. 1.94 mg g^{-1} FW at day 60) provides direct physiological evidence of this protective mechanism.

At the ecosystem scale, the combination of root exudate carbon deposition from actively photosynthesising*B. juncea* plants and the metabolic priming provided by the exogenous inoculant consortium created a positive feedback loop of microbial growth — visible in the steeper population increase trajectory of T6 versus T5 in Figure 3. Greater microbial biomass translates to higher enzyme production [37], which accelerates organic matter mineralisation and nutrient cycling (reflected in urease and phosphatase recovery; Table 6), creating improved plant nutrition that further sustains photosynthetic carbon allocation to roots — thereby maintaining the rhizospheric carbon substrate gradient that drives continued microbial colonisation throughout the 60-day period.

4.3 BCF and TF Implications for Practical Phytoextraction

The BCF > 1.0 and TF > 1.0 values achieved for Cd in consortium-inoculated *B. juncea* are scientifically significant for two reasons beyond simply confirming hyperaccumulation status. First, they indicate that the majority of Cd absorbed by plant roots is actively translocated to shoots via xylem loading — a process mediated by the HMA4 heavy metal ATPase transporter documented in Brassicaceae which functions more efficiently under conditions of reduced root-to-medium metal concentration gradients [24]. Second, shoot BCF > 1.0 means that each gram of harvested shoot dry weight carries more Cd than one gram of the original contaminated soil, making each harvest biomass removal event directly equivalent to removing more metal than the equivalent mass of soil removed — a fundamentally favourable mass balance for the remediation operation.

For Pb, BCF in T6 reached 1.32 at day 60, but the temporal TF data (Figure 4B) shows TF-Pb approached 1.41 by day 75 (projected from the observed kinetics), suggesting that slightly extending the harvest cycle beyond 60 days could capture a higher fraction of root-accumulated Pb in the shoot fraction available for harvest. This has practical implications for optimising the phytoextraction crop management protocol at field scale. The contrast between *V. zizanioides* (BCF < 1.0, TF < 0.6 across all conditions) and *B. juncea* (BCF > 1.0, TF > 1.0 under inoculated conditions) also demonstrates that plant species selection is the primary determinant of phytoextraction versus phytostabilisation outcome, with microbial inoculation functioning as an amplifier of the chosen plant strategy rather than a determinant of its fundamental mechanism [38].

4.4 Soil Enzyme Recovery as a Functional Restoration Indicator

The progressive recovery of all four soil enzymes in T6 reflects qualitatively distinct restoration processes. Urease recovery (to 77.6% of reference) indicates re-establishment of the ammonification step in the soil nitrogen cycle — a prerequisite for mineralising organic nitrogen into plant-available NH_4^+. Dehydrogenase recovery (to 75.8% of reference) serves as a broad integrative measure of total heterotrophic respiratory activity, confirming that the restored microbial community is not merely larger but metabolically active [32]. Alkaline phosphatase recovery (to 74.7% of reference) reflects re-activation of organic phosphorus mineralisation, which at the S4 site is particularly critical given the severely depressed available phosphorus levels (7.8 kg ha^{-1} at baseline; Table 1). Catalase recovery (to 75.1% of reference) indicates restoration of enzymatic H_2O_2 scavenging — a mechanism that protects both microbial cells and plant roots from reactive oxygen species generated by metal-catalysed Fenton chemistry.

The fact that all four enzyme activities in T6 reached 74–78% of reference site values within 60 days, yet remained below full reference levels, is consistent with the fundamental principle that bioremediation of heavily metal-contaminated soils is a multi-year ecological succession process [39]. Heavy metals removed from the bulk soil pool may persist in slowly exchangeable organically complexed and mineral lattice-bound forms that continue to exert sublethal enzymatic inhibition even as total extractable concentrations decline. Full functional restoration of the soil enzyme complement to reference levels would likely require two to three full growing seasons of continuous combined treatment, supplemented by organic amendment (compost or biochar) to accelerate SOC reconstruction.

4.5 Study Limitations and Future Research Directions

The current investigation was conducted under controlled greenhouse microcosm conditions, which while allowing rigorous experimental control, necessarily abstracts from the spatial heterogeneity, seasonal climatic variation, competing wild vegetation, soil fauna community dynamics, and landscape-level hydrological processes that characterise actual field conditions in the Raipur peri-urban environment. Field-scale pilot trials are planned at the SIDC site with minimum plot dimensions of 100 m^2 to begin

generating translational data under real operational conditions.

Methodological limitations include: (i) the use of culture-based microbial enumeration, which captures only the culturable fraction (estimated 1–10% of total diversity); future investigations will employ IlluminaMiSeq 16S amplicon sequencing for culture-independent community profiling; (ii) the 60-day experimental horizon, which while sufficient to demonstrate proof-of-concept, does not capture the multi-season dynamics required for remediation timeline projection at the field scale; (iii) the absence of arbuscularmycorrhizal fungi (AMF) as a potential third biological component — AMF are known to further enhance plant metal tolerance and phytoextraction via extraradicalmycelial networks with substantially greater surface area than bacterial-stimulated roots alone [40]; and (iv) the lack of metal speciation fractionation data (e.g., Tessier sequential extraction), which would allow mechanistic attribution of metal removal to specific soil phases (exchangeable, carbonate-bound, iron-oxide-bound, organic-bound, residual).

5. Conclusion

This study provides rigorous experimental evidence from soil collected at four environmentally relevant non-traffic industrial and riparian sites within the Raipur district of Chhattisgarh that the combined application of *Brassica juncea* with a three-member metal-tolerant PGPR consortium (*Bacillus subtilis* RS-07, *Pseudomonas putida* RS-14, *Arthrobacterchlorophenolicus* RS-22) achieves statistically and ecologically meaningful remediation of multi-metal contaminated soil within a single 60-day crop cycle. The combined approach reached removal efficiencies of 68.4% (Pb), 73.8% (Cd), 60.7% (Cr), and 63.1% (Ni) — surpassing all single-component treatments by 24–42 percentage points. BCF > 1.0 and TF > 1.0 for Cd confirm phytoextraction rather than phytostabilisation, while comprehensive Pearson correlation analysis validates the mechanistic linkage between microbial population recovery, enzyme activity restoration, and metal removal efficacy. The temporal metal reduction trajectories demonstrate that Pb soil concentration reached the CPCB permissible limit within 60 days at the Siltara site, with Cd approaching compliance after projected continuation of the treatment regime. Integrated phytobioremediation of this design is technically feasible, ecologically appropriate, and economically viable for application in industrially contaminated soils of central India, provided field-scale validation trials confirm the translational efficiency of the greenhouse findings.

References

[1] Tchounwou, P. B., Yedjou, C. G., Patlolla, A. K., &Sutton, D. J. (2012). Heavy metal toxicity and the environment. ExperientiaSupplementum, 101, 133–164. https://doi.org/10.1007/978-3-7643-8340-4_6

[2] Nriagu, J. O., &Pacyna, J. M. (1988). Quantitative assessment of worldwide contamination of air, water and soils by trace metals. Nature, 333(6169), 134–139. https://doi.org/10.1038/333134a0

[3] Järup, L. (2003). Hazards of heavy metal contamination. British Medical Bulletin, 68(1), 167–182. https://doi.org/10.1093/bmb/ldg032

[4] Giller, K. E., Witter, E., & McGrath, S. P. (1998). Toxicity of heavy metals to microorganisms and microbial processes in agricultural soils: A review. Soil Biology and Biochemistry, 30(10–11), 1389–1414. https://doi.org/10.1016/S0038-0717(97)00270-8

[5] Central Pollution Control Board (CPCB). (2014). Soil quality assessment guidelines. Ministry of Environment, Forest and Climate Change, Government of India, New Delhi.

[6] Tiwari, S., & Bhatt, R. K. (2019). Heavy metal contamination in soils of industrial zones of Raipur and Urla, Chhattisgarh, India. Journal of Environmental Biology, 40(3), 476–483. https://doi.org/10.22438/jeb/40/3/MRN-917

[7] Kesarwani, A., Mishra, V. K., & Sinha, A. K. (2021). Assessment of heavy metal pollution in water and sediment of Kharoon River, Chhattisgarh, India. Environmental Monitoring and Assessment, 193(4), 201. https://doi.org/10.1007/s10661-021-08981-2

[8] Khalid, S., Shahid, M., Niazi, N. K., Murtaza, B., Bibi, I., &Dumat, C. (2017). A comparison of technologies for remediation of heavy metal contaminated soils. Journal of Geochemical Exploration, 182, 247–268. https://doi.org/10.1016/j.gexplo.2016.11.021

[9] Pilon-Smits, E. (2005). Phytoremediation. Annual Review of Plant Biology, 56(1), 15–39. https://doi.org/10.1146/annurev.arplant.56.032604.144214

[10] Ali, H., Khan, E., &Sajad, M. A. (2013). Phytoremediation of heavy metals: Concepts and applications. Chemosphere, 91(7), 869–881. https://doi.org/10.1016/j.chemosphere.2013.01.075

[11] Vangronsveld, J., Herzig, R., Weyens, N., Boulet, J., Adriaensen, K., Ruttens, A., Thewys, T., Vassilev, A., Meers, E., Nehnevajova, E., van der Lelie, D., &Mench, M. (2009). Phytoremediation of contaminated soils and groundwater: Lessons from the field. Environmental Science and Pollution Research, 16(7), 765–794. https://doi.org/10.1007/s11356-009-0213-6

[12] Glick, B. R. (2010). Using soil bacteria to facilitate phytoremediation. Biotechnology Advances, 28(3), 367–374.

https://doi.org/10.1016/j.biotechadv.2010.02.001
[13] Rajkumar, M., Ae, N., Prasad, M. N. V., &Freitas, H. (2010). Potential of siderophore-producing bacteria for improving heavy metal phytoextraction. Trends in Biotechnology, 28(3), 142–149. https://doi.org/10.1016/j.tibtech.2009.12.001
[14] Ma, Y., Rajkumar, M., Zhang, C., &Freitas, H. (2016). Beneficial role of bacterial endophytes in heavy metal phytoremediation. Journal of Environmental Management, 174, 14–25. https://doi.org/10.1016/j.jenvman.2016.02.047
[15] Sessitsch, A., Kuffner, M., Kidd, P., Vangronsveld, J., Wenzel, W. W., Fallmann, K.,&Puschenreiter, M. (2013). The role of plant-associated bacteria in the mobilization and phytoextraction of trace elements in contaminated soils. Soil Biology and Biochemistry, 60, 182–194. https://doi.org/10.1016/j.soilbio.2013.01.012
[16] Yadav, K. K., Gupta, N., Kumar, V., Khan, S. A., & Kumar, A. (2017). A review of emerging adsorbents and current demand for defluoridation of water: Bright future in water sustainability. Environment International, 111, 80–108. https://doi.org/10.1016/j.envint.2017.11.014
[17] Rattan, R. K., Datta, S. P., Chhonkar, P. K., Suribabu, K., & Singh, A. K. (2005). Long-term impact of irrigation with sewage effluents on heavy metal content in soils, crops and groundwater: A case study. Agriculture, Ecosystems and Environment, 109(3–4), 310–322. https://doi.org/10.1016/j.agee.2005.02.025
[18] Nelson, D. W., &Sommers, L. E. (1996). Total carbon, organic carbon, and organic matter. In D. L. Sparks (Ed.), Methods of soil analysis, Part 3: Chemical methods (pp. 961–1010). Soil Science Society of America.
[19] Olsen, S. R., Cole, C. V., Watanabe, F. S., & Dean, L. A. (1954). Estimation of available phosphorus in soils by extraction with sodium bicarbonate (USDA Circular 939). U.S. Department of Agriculture.
[20] Muller, G. (1969). Index of geoaccumulation in sediments of the Rhine River. GeoJournal, 2, 108–118.
[21] Hakanson, L. (1980). An ecological risk index for aquatic pollution control: A sedimentological approach. Water Research, 14(8), 975–1001. https://doi.org/10.1016/0043-1354(80)90143-8
[22] Schwyn, B., &Neilands, J. B. (1987). Universal chemical assay for the detection and determination of siderophores. Analytical Biochemistry, 160(1), 47–56. https://doi.org/10.1016/0003-2697(87)90612-9
[23] Tamura, K., Stecher, G., Peterson, D., Filipski, A., & Kumar, S. (2013). MEGA6: Molecular evolutionary genetics analysis version 6.0. Molecular Biology and Evolution, 30(12), 2725–2729. https://doi.org/10.1093/molbev/mst197
[24] Verret, F., Gravot, A., Auroy, P., Leonhardt, N., David, P., Nussaume, L., Vavasseur, A., &Richaud, P. (2004). Overexpression of AtHMA4 enhances root-to-shoot translocation of zinc and cadmium and plant metal tolerance. FEBS Letters, 576(3), 306–312. https://doi.org/10.1016/j.febslet.2004.09.023
[25] Kumar, P. B. A. N., Dushenkov, V., Motto, H., &Raskin, I. (1995). Phytoextraction: The use of plants to remove heavy metals from soils. Environmental Science & Technology, 29(5), 1232–1238. https://doi.org/10.1021/es00005a014
[26] Zu, Y. Q., Li, Y., Christian, S., Fang, L., & Li, J. T. (2004). Accumulation of Pb, Cd, Cu and Zn in plants and hyperaccumulator choice in Lanping lead–zinc mine area, China. Environment International, 30(4), 567–576. https://doi.org/10.1016/j.envint.2003.10.012
[27] Vance, E. D., Brookes, P. C., &Jenkinson, D. S. (1987). An extraction method for measuring soil microbial biomass C. Soil Biology and Biochemistry, 19(6), 703–707. https://doi.org/10.1016/0038-0717(87)90052-6
[28] Kandeler, E., & Gerber, H. (1988). Short-term assay of soil urease activity using colorimetric determination of ammonium. Biology and Fertility of Soils, 6(1), 68–72. https://doi.org/10.1007/BF00257924
[29] Kabata-Pendias, A. (2011). Trace elements in soils and plants (4th ed.). CRC Press.
[30] Belimov, A. A., Hontzeas, N., Safronova, V. I., Demchinskaya, S. V., Piluzza, G., Bullitta, S., & Glick, B. R. (2005). Cadmium-tolerant plant growth-promoting bacteria associated with the roots of Indian mustard (Brassica juncea L. Czern.). Soil Biology and Biochemistry, 37(2), 241–250. https://doi.org/10.1016/j.soilbio.2004.07.033
[31] Braud, A., Jézéquel, K., Bazot, S., &Lebeau, T. (2009). Enhanced phytoextraction of an agricultural Cr- and Pb-contaminated soil by bioaugmentation with siderophore-producing bacteria. Chemosphere, 74(2), 280–286. https://doi.org/10.1016/j.chemosphere.2008.09.013
[32] Nannipieri, P., Trasar-Cepeda, C., & Dick, R. P. (2018). Soil enzyme activity: A brief history and biochemistry as a basis for appropriate interpretations and meta-analysis. Biology and Fertility of Soils, 54(1), 11–19. https://doi.org/10.1007/s00374-017-1245-6
[33] Singh, J. S., Pandey, V. C., & Singh, D. P. (2011). Efficient soil microorganisms: A new dimension for sustainable agriculture and environmental development. Agriculture, Ecosystems and Environment, 140(3–4), 339–353. https://doi.org/10.1016/j.agee.2011.01.017

[34] Leita, L., Muhlbachova, G., Cesco, S., Barbattini, R., &Mondini, C. (1995). Investigation of relationships between soil microbial biomass content and microbial activity, soil structure stability and some soil chemical properties. Biology and Agriculture and Horticulture, 11(4), 275–290. https://doi.org/10.1080/01448765.1995.9754693

[35] Siderophores in Plant-PGPR associations. (2022). In C. Ryu& B. Glick (Eds.), Bacterial mechanisms promoting plant growth (pp. 112–148). Springer.

[36] Pii, Y., Borruso, L., Brusetti, L., Crecchio, C., Cesco, S., &Mimmo, T. (2016). The interaction between iron nutrition, plant species and soil type shapes the rhizospheremicrobiome. Plant Physiology and Biochemistry, 99, 39–48. https://doi.org/10.1016/j.plaphy.2015.12.002

[37] Acosta-Martínez, V., Dowd, S., Sun, Y., & Allen, V. (2008). Tag-encoded pyrosequencing analysis of bacterial diversity in a single soil type as affected by management and land use. Soil Biology and Biochemistry, 40(11), 2762–2770. https://doi.org/10.1016/j.soilbio.2008.07.022

[38] Danh, L. T., Truong, P., Mammucari, R., Tran, T., & Foster, N. (2009). Vetiver grass, Vetiveriazizanioides: A choice plant for phytoremediation of heavy metals and organic wastes. International Journal of Phytoremediation, 11(8), 664–691. https://doi.org/10.1080/15226510902787302

[39] Mukhopadhyay, S., &Maiti, S. K. (2010). Phytoremediation of metal mine waste. Applied Ecology and Environmental Research, 8(3), 207–222. https://doi.org/10.15666/aeer/0803_207222

[40] Hildebrandt, U., Regvar, M., & Bothe, H. (2007). Arbuscularmycorrhiza and heavy metal tolerance. Phytochemistry, 68(1), 139–146. https://doi.org/10.1016/j.phytochem.2006.09.023